CRITICAL COMPARISON OF MASS TRANSFER MODELS FOR INTERNALLY–CONTROLLED SCF EXTRACTION OF SOLID SUBSTRATES

José Manuel del Valle[1,*] & Edgar Uquiche[2]

[1] Pont. Univ. Católica de Chile, Avda. Vicuña Mackenna 4860, Macul, Santiago, Chile.

[2] Univ. de La Frontera, Avda. Francisco Salazar 01145, Temuco, Chile.

[*] Fax: (56 2) 354 5803. E-mail: delvalle@ing.puc.cl.

Three models for the supercritical fluid (SCF) extraction of solids with different internal mass transfer mechanism were critically compared in this work. Internal mass transfer hypothesis included: transient diffusion; linear driving force (LDF); and desorption-dissolution-diffusion (DDD). A sensitivity analysis was performed on the basis of Biot number (Bi –ratio between internal and external mass transfer resistances–) and characteristic external extraction time (τ_e –ratio between the external mass transfer resistance and residence time of the SCF in the extractor–). The negative effect of a 2-order of magnitude increase in Bi (1–100) in decreasing extraction rates was equivalent to that of a one-order of magnitude increase in τ_e (0.1–1). The LDF approximation could be used for the two other models under analysis if the total compounded porosity of the bed (ε) and particles (ε_p) was considered, a model-dependent definition of Bi was utilized ($Bi=k_fR/D_sK$ for Fickean and LDF model, $Bi'=k_fR/D_p$ for DDD model), and the values of Bi were <100. The LDF model was applied to literature data on essential oil extraction from lavender flowers and pennyroyal leaves with supercritical carbon dioxide (SC-CO_2) at 100 bar and 50 °C. Analysis of interstitial solvent velocity effects suggested that the convective mass transfer coefficient in the SCF is smaller than predicted by dimensionless correlations for packed beds operating with SCFs.

INTRODUCTION

Mass transfer parameters derived from data generated in a laboratory or pilot plant unit can aid in the scaling-up and design of industrial SCF extraction processes for solid substrates [1]. Parameter evaluation, in turn, depends on the implementation of appropriate mass transfer models for packed beds. Unfortunately, since models with different hypothesis about the limiting mass transfer mechanism can describe typical cumulative extraction plots (recovered solute *versus* extraction time) for botanical substrates treated with SCFs, it is difficult to discriminate between models based on their fitting capabilities for experimental data [1]. In this work, we expanded a previous contribution by considering alternative internal mass transfer mechanisms proposed in specialized literature. Hypotheses included Fickean [1] or parabolic concentration profiles of residual solute in the solid matrix [2], and a desorption-dissolution-diffusion mechanism [3].

MATHEMATICAL MODELS

Fickean model. This corresponds to the general model of del Valle *et al.* [1]. A differential mass balance equation was written for the SCF surrounding spherical particles of solid substrate in a packed bed (eqn. 1). The flux of solute transferred from the solid to the SCF (J) was estimated using equation 2, which assumes a constant partition coefficient of pseudo-solute ($K=C_s/C_f^*$) between the solid matrix and SCF. Equation 3 represents solute

diffusion within the solid particles, and finally, equations 4a-e represent the initial and boundary conditions of the system.

$$\frac{\partial C_f}{\partial t} + u\frac{\partial C_f}{\partial z} = \frac{1-\varepsilon}{\varepsilon} J \tag{1}$$

$$J\big|_{z,t} = \frac{3k_f}{R}\left(\frac{C_s\big|_{r=R,z,t}}{K} - C_f\big|_{z,t}\right) \tag{2}$$

$$\frac{\partial C_s}{\partial t} = D_s\left(\frac{\partial^2 C_s}{\partial r^2} + \frac{2}{r}\frac{\partial C_s}{\partial r}\right) \tag{3}$$

$$C_f\big|_{z,t=0} = 0 \tag{4a}$$

$$C_f\big|_{z=0,t} = 0 \tag{4b}$$

$$C_s\big|_{r,z,t=0} = C_{so} \tag{4c}$$

$$\left.\frac{\partial C_s}{\partial r}\right|_{r=0,z,t} = 0 \tag{4d}$$

$$-D_s\left.\frac{\partial C_s}{\partial r}\right|_{r=R,z,t} = k_f\left(\frac{C_s\big|_{r=R,z,t}}{K} - C_f\big|_{z,t}\right) \tag{4e}$$

LDF model. Mass balance equation 1 applies in this case also. However, when the concentration profile of residual solute in the solid matrix is assumed to be parabolic, definition 2 and differential equation 3 can be replaced by equations 5 and 6, respectively [2]. In this case only average solute concentrations in the solid matrix ($\overline{C}_s$) are of interest. Initial condition 4a and boundary condition 4b were maintained in this case, and initial/boundary conditions 4c-e were replaced by equation 7.

$$J = \frac{15k_f D_s K}{k_f R^2 + 5D_s KR}\left(\frac{\overline{C}_s}{K} - C_f\right) \tag{5}$$

$$\frac{\partial \overline{C}_s}{\partial t} = -J \tag{6}$$

$$\overline{C}_s\big|_{z,t=0} = C_{so} \tag{7}$$

DDD model. This model was described by in detail by Goto *et al.* [3]. Mass balance equation 1 applies, but a distinction is made in this case between the solute bound to the solid matrix (C_s) and in its pores (C_p), which are related by desorption kinetics. However, it was assumed that equilibrium is established instantaneously in the pores due to relatively fast desorption, which can be characterized by a constant partition coefficient of solute ($K=C_s/C_p^*$) between the solid matrix and fluid phase within the pores. Under these assumptions, definition 2 and differential equation 3 were replaced by equations 8 and 9, respectively. Initial condition 4a and boundary condition 4b were also maintained in this case, but initial/boundary conditions 4c-e were replaced by equations 10a-c.

$$J\big|_{z,t} = \frac{3k_f}{R}\left(C_p\big|_{r=R,z,t} - C_f\big|_{z,t}\right) \tag{8}$$

$$\frac{\partial C_p}{\partial t} = \frac{D_p}{\varepsilon_p + K(1-\varepsilon_p)}\left(\frac{\partial^2 C_p}{\partial r^2} + \frac{2}{r}\frac{\partial C_p}{\partial r}\right) \tag{9}$$

$$C_p\Big|_{r,z,t=0} = C_{po} \tag{10a}$$

$$\left.\frac{\partial C_p}{\partial r}\right|_{r=0,z,t} = 0 \tag{10b}$$

$$-D_p\left.\frac{\partial C_s}{\partial r}\right|_{r=R,z,t} = k_f\left(C_p\Big|_{r=R,z,t} - C_f\Big|_{z,t}\right) \tag{10c}$$

SENSITIVITY ANALYSIS

The Fickean and LDF models were re-written in terms of a dimensionless time [θ (=t u/H) = 0], axial position [0 = ξ (=z/H) = 1], radial position [0 = δ (=r/R) = 1], and solute concentration in the SCF [0 = Y (=K C_f/C_{so}) = 1] and solid phase [0 = X (=C_s/C_{so}) = 1; 0 = $\overline{X}$ (=$\overline{C}_s/C_{so}$) = 1]. On the on other hand, dimensionless concentrations for the DDD model were re-defined as: $Y=C_f/C_o$, for the SCF phase; $Y_p=C_p/C_o$, for the fluid phase within the pores; and $X=C_s/C_o$, for the solid phase, where $C_o= K' C_{so}/K$ and $K'=\varepsilon_p+K(1-\varepsilon_p)$. Table 1 summarizes the dimensionless differential mass balance equations, initial conditions, and boundary conditions for the two phases and the three models.

Close examination suggests that the solutions of the differential equations in Table 1 depend on the partition of solute between the phases (K, K'), bed and particle porosity (ε, ε_p) and two dimensionless parameters, namely: i) Biot number ($Bi=k_fR/D_sK$ for Fickean and LDF model, $Bi'=k_fR/D_p$ for DDD model), which represents the ratio between internal and external mass transfer resistances; and, ii) characteristic external extraction time ($\tau_e=u/k_fa_pH$, where $a_p=3/R$), which represents the ratio between the external resistance to mass transfer and the residence time of the SCF in the extractor. A sensitivity analysis was performed on the basis of Bi and τ_e, which is summarized in Figure 1 for the LDF model (the base case was: K=20, ε=0.6, Bi=10, and τ_e=0.1). Extraction rates increased as a result of a decrease in either Bi or τ_e, but the effect of a one-order of magnitude change in τ_e (0.1-1) was similar to that of a 2-order of magnitude change in Bi (1-100). del Valle *et al.* [1] studied the effect of variations in K and ε by means of another dimensionless parameter (Γ=ε/(1-ε)K) that is related to the partition of solute between the SCF and solid phases under equilibrium conditions, and concluded that as Γ increases (and the solute is more tightly held by the solid matrix), the amount of solute carried out by the SCF decreases, thus increasing extraction times.

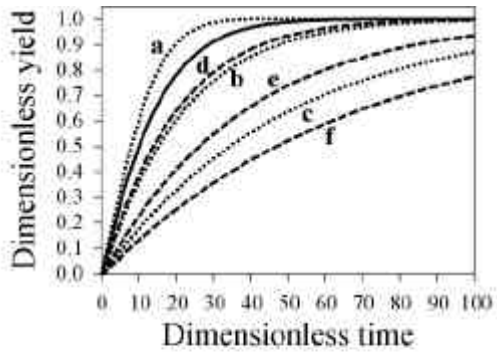

Figure 1. Dimensionless cumulative extraction plots for LDF model. Continuous line: base case (Bi=10, τ_e=0.1). Dotted lines: sensitivity analysis for Bi (**a**: Bi=1; **b**: Bi=30; **c**: Bi=100, τ_e=0.1). Segmented lines: sensitivity analysis for τ_e (**d**: τ_e=0.2; **e**: τ_e=0.5; **f**: τ_e=1, Bi=10).

Table 1. Dimensionless differential mass balance equations, initial conditions, and boundary conditions for the SCF phase and solid matrix phases for the Fickean, LDF and DDD models.

Model	SCF phase	Solid phase / Pores within solid phase
Fickean	$\frac{\partial Y}{\partial \theta}+\frac{\partial Y}{\partial \xi}=\frac{1-\varepsilon}{\varepsilon}\frac{1}{\tau_e}(X-Y)$ $Y\big\vert_{\xi,\theta=0}=0$ $Y\big\vert_{\xi=0,\theta}=0$	$\frac{\partial X}{\partial \theta}=\frac{1}{3K\tau_e Bi}\left(\frac{\partial^2 X}{\partial \delta^2}+\frac{2}{\delta}\frac{\partial X}{\partial \delta}\right)$ $X\big\vert_{\delta,\xi,\theta=0}=1$ $\left.\frac{\partial X}{\partial \delta}\right\vert_{\delta=0,\xi,\theta}=0$ $\left.\frac{\partial X}{\partial \delta}\right\vert_{\delta=1,\xi,\theta}=-Bi\left(X\big\vert_{\delta=1,\xi,\theta}-Y\big\vert_{\xi,\theta}\right)$
LDF	$\frac{\partial Y}{\partial \theta}+\frac{\partial Y}{\partial \xi}=\frac{1-\varepsilon}{\varepsilon}\frac{1}{\tau_e}\frac{5}{Bi+5}(\overline{X}-Y)$ $Y\big\vert_{\xi,\theta=0}=0$ $Y\big\vert_{\xi=0,\theta}=0$	$\frac{\partial \overline{X}}{\partial \theta}=-\frac{1}{\tau_e}\frac{5}{Bi+5}(\overline{X}-Y)$ $\overline{X}\big\vert_{\xi,\theta=0}=1$
DDD	$\frac{\partial Y}{\partial \theta}+\frac{\partial Y}{\partial \xi}=\frac{1-\varepsilon}{\varepsilon}\frac{1}{\tau_e}(Y_p-Y)$ $Y\big\vert_{\xi,\theta=0}=0$ $Y\big\vert_{\xi=0,\theta}=0$	$\frac{\partial X}{\partial \theta}=\frac{1}{3K_1'\tau_e Bi'}\left(\frac{\partial^2 Y_p}{\partial \delta^2}+\frac{2}{\delta}\frac{\partial Y_p}{\partial \delta}\right)$ $X\big\vert_{\delta,\xi,\theta=0}=\frac{K_1}{K_1'}$ $Y_p\big\vert_{\delta,\xi,\theta=0}=\frac{1}{K_1'}$ $\left.\frac{\partial Y_p}{\partial \delta}\right\vert_{\delta=1,\xi,\theta}=-Bi'\left(Y_p\big\vert_{\delta=1,\xi,\theta}-Y\big\vert_{\xi,\theta}\right)$

Figure 2 compares predictions of the Fickean, LDF and DDD models for two combinations of Bi and τ_e. Solute partition between the phases (K=20) and total porosity ($\varepsilon_T=\varepsilon+\varepsilon_p(1-\varepsilon)=0.6$) were kept constant in all cases. Two values of particle porosity were also compared for the DDD model (ε_p=0.2 and 0.375) that resulted in different values of bed porosity (ε=0.5 and 0.375, respectively). Predicted cumulative extraction plots were virtually the same for the three models under analysis for fast extractions (Fig. 2A), and small differences were observed for slow extractions (Fig. 2B). The LDF approximation was inappropriate for $\theta<60$. This is in agreement with Do & Rice [4], who showed that residual radial solute concentration profiles can be assumed to be parabolic in shape only when $\theta/Bi\tau_e=3$ ($\theta/Bi\tau_e=6$ in Fig. 2B). On the other hand, Goto *et al.* [3] suggested that the LDF is appropriate only when Bi<10. Figure 2B also suggests that extraction rate improves slightly as a result of an increase in ε_p for long extraction times. It can be concluded that the LDF approximation can be applied for the two other models under analysis provided that the total porosity of the bed and particles (ε_T) is considered, that a model-dependent

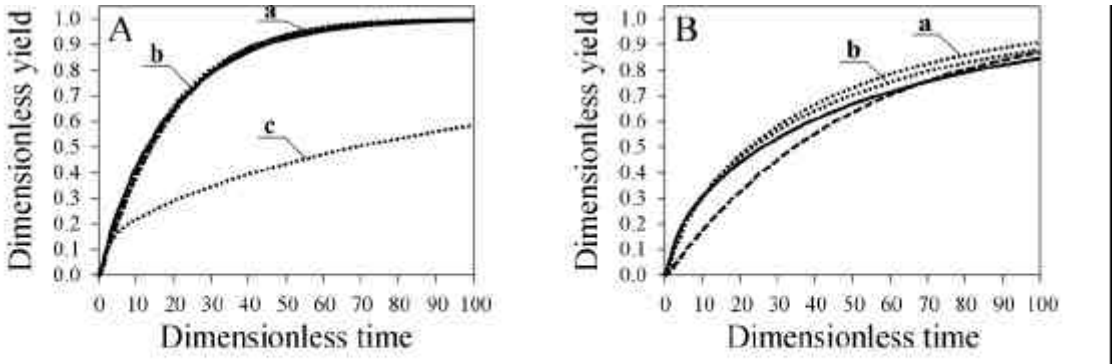

Figure 2. Comparative dimensionless cumulative extraction plots for: (**A**) Bi=10 and τ_e=0.2; or, (**B**) Bi=100 and τ_e=0.1. Continuous lines: Fickean model. Segmented lines: LDF model. Dotted lines: DDD model for: (**a**) ε_p=0.375; (**b**) ε_p=0.2; and, (**c**) ε_p=0.2 and alternative definition of Bi.

used, and that values of Bi are not too large. To illustrate the effect of the definition of Bi, an additional simulated extraction plot is included in Figure 2A for the DDD model and K=20, ε_p=0.2, ε=0.5, τ_e=0.2, and $Bi^{'}$=200 (corresponding to Bi=k_fR/D_sK=10).

FITTING OF LITERATURE DATA

The use of the LDF model for fitting experimental cumulative extraction plots is illustrated in Figure 3 for selected literature data on essential oil extraction with SC-CO_2. Data correspond to studies on the effect of solvent ratio for the extraction of camphor and fenchone from lavender (*Lavandula stoechas* subspecies *C. Boiss*) flowers [5], and of essential oils from pennyroyal (*Mentha pulegium* L.) leaves [6]. Both sets of experiments were performed with SC-CO_2 at 100 bar and 50 ºC. Partition parameters (K) were estimated by plotting the essential oil yield *versus* specific solvent consumption for each one of the two experimental sets, and calculating the slope of the initial straight portion [7]. Values of K were 7.6 for lavender, and 16.6 for pennyroyal. We proceeded to estimate best-fit values of k_p, $5k_fD_eK/(k_fR+5D_eK)$, for each condition. Dimensionless correlations for the convective mass transfer coefficient in the SCF phase (k_f) have the general form:

$$N_{Sh} = a\,(N_{Re})^n\,(N_{Sc})^{0.33} \qquad (11)$$

where N_{Sh} ($2k_fR/D$) is the dimensionless Sherwood number, N_{Re} ($2\rho UR/\mu$), the dimensionless Reynolds number, and N_{Sc} ($\mu/\rho D$), the dimensionless Schmidt number. The physical properties of the loaded SCF phase (ρ, μ, D) were estimated using the procedure proposed by del Valle *et al.* [8] using PM=885.4 g/mol and V_c=3200 cm^3/mol for a typical solute in plant essential oils [7]. When the solvent conditions remain unchanged, equation 11 reduces to:

$$k_f = a^{'}\,U^n\,R^{n-1} \qquad (12)$$

In a second stage, best-fit values of k_p for each experiment were used to determine best fit values of $a^{'}$ (0.89), n (1.82), and substrate-dependent D_e (2.5×10^{-9} m^2/s for lavender, 3×10^{-9} m^2/s for pennyroyal). Values of 'n' in dimensionless correlations for mass transfer coefficients in packed beds range from 0.6 [9] and 0.83 [10]. Best-fit values of k_f estimated using the aforementioned procedure ranged $0.84–4.3\times10^{-6}$ m/s, which are about 10 times smaller than predicted using the correlation of Tan *et al.* [10], which has been suggested for

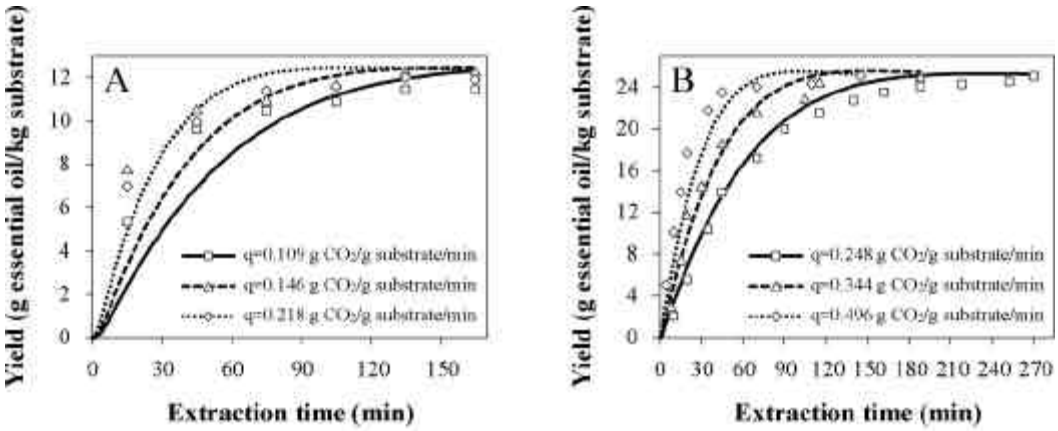

Figure 3. Effect of solvent ratio (q) on cumulative extraction plots of essential oils from: (**A**) Lavender flowers (data source: [5]); and, (**B**) Pennyroyal leaves (data source: [6]). All experiments were performed with SC-CO_2 at 100 bar and 50 °C.

the extraction of vegetable substrates with SC-CO2 in a packed bed [8]. Model fitting was obviously worst for the data of Akgün *et al.* [5] than that of Reis-Vasco *et al.* [6] (*cf.* Fig. 3). The values of Bi ranged from 0.30 to 1.0 for lavender flowers and from 0.07 to 0.25 for pennyroyal leaves, for which the LDF approximation is adequate regardless of the internal mass transfer mechanism.

Acknowledgements

Funding by Fondecyt (project 103-0735) from Chile is greatly acknowledged.

REFERENCES

[1] DEL VALLE, J.M., NAPOLITANO, P., FUENTES, N., Ind. Eng. Chem. Res., 39, **2000**, p. 4720
[2] PEKER, H., SRINIVASAN, M.P., SMITH, J.M., McCOY, B.J., AIChE J., 38, **1992**, p. 761
[3] GOTO, M., ROY, B.C., KODAMA, A., HIROSE, T., J. Chem. Eng. Japan, 31, **1998**, p. 171
[4] DO, D.D., RICE, R.G., AIChE J., 32, **1986**, p. 149
[5] AKGÜN, M., AKGÜN, N.A., DINÇER, S., Ind. Eng. Chem. Res. 39, **2000**, p. 473
[6] REIS-VASCO, E.M.C., COELHO, J.A.P., PALAVRA, A.M.F., MARRONE, C., REVERCHON, E., Chem. Eng. Sci. 55, **2000**, p. 2917
[7] REVERCHON, E., MARRONE, C., Chem. Eng. Sci. 52, **1997**, p. 3421
[8] DEL VALLE, J.M., RIVERA, O., MATTEA, M., RUETSCH, L., DAGHERO, J., FLORES, A., J. Supercrit. Fluids (submitted)
[9] WAKAO, N., KAGUEI, S., Heat and Mass Transfer in Packed Beds, Gordon and Breach: New York, **1982**
[10] TAN, C.-S., LIANG, S.-K., LIOU, D.-C., Chem. Eng. J. 38, **1988**, p. 17